Relevance of the Hölderian regularity-based interpolation for range-Doppler ISAR image post-processing

Vincent Corretja [1, 2], Pierrick Legrand [3], Eric Grivel [2] and Jacques Levy-Vehel [4]

THALES SYSTEMES AEROPORTES S.A.
[1] 16, avenue Gustave Eiffel, 33600 PESSAC, FRANCE

[2] Université Bordeaux 1 – IPB ENSEIRB-MATMECA – IMS – UMR CNRS 5218
[3] Université Bordeaux Segalen - ALEA Team - INRIA Bordeaux Sud-Ouest – IMB – UMR CNRS 5251
351, cours de la Libération, 33405 TALENCE CEDEX, FRANCE

[4] INRIA - B.P. 105, 78153 Le Chesnay cedex, France

vincent.corretja@fr.thalesgroup.com, pierrick.legrand@u-bordeaux2.fr
eric.grivel@ims-bordeaux.fr, jacques.levy-vehel@inria.fr

Abstract

In ISAR processing, post-processing of the range Doppler image is useful to help the practitioner for ship recognition. Among the image post-processing tools, interpolation methods can be of interest especially when zooming. In this paper, we study the relevance of the Hölderian regularity-based interpolation. In that case, interpolating consists in adding a new scale in the wavelet transform and the new wavelet coefficients can be estimated from others. In the original method, initially proposed by two of the authors, the image is first interpolated along the rows and then along the columns. Concerning the diagonal pixels, they are estimated as the mean of the adjacent original and interpolated pixels. Here, we propose a variant where the diagonal pixels are estimated by taking into account the local orientation of the image. It has the advantage of conserving local regularity on all interpolated pixels of the image. A comparative study on synthetic data and real range-Doppler images is then carried out with alternative interpolation techniques such as the linear interpolation, the bicubic one, the nearest neighbour interpolation, etc. The simulation results confirm the effectiveness of the approach.

Keywords: Inverse synthetic aperture radar, range-Doppler image, interpolation, Hölder exponent, local regularity.

1. Introduction

High-resolution radar images can be obtained by using synthetic aperture radar (SAR) and inverse synthetic aperture radar (ISAR). Both are key tools for civil and defence applications. SAR is usually used to map the land whereas ISAR is used for moving objects detection and recognition, by taking advantage of the target rotational motion with respect to the radar line of sight.

In radar processing, pulse radar sends out short bursts. The distance between the radar and the ship can be deduced by measuring the time taken by the radar wave to go to the ship and to come back. For each emitted pulse sent periodically, the collected backscattered signals are associated to range bins. In ISAR processing, this leads to a two-dimensional (2-D) signal, where one dimension corresponds to the ranges under study and the other dimension corresponds to the response of each emitted pulse. This 2-D signal is the input signal of the processing chain. The purpose is to obtain a range-Doppler image, which is a representation of the Doppler frequency variations –due to the relative target rotational motion– according to the distance between the radar and the area under study. Then, the practitioner uses this image for ship recognition and classification. Consequently, the main objective of ISAR processing is to obtain a range-Doppler image that is as "clear" as possible, i.e. an image that is not "too" blurred and that is not "too" disturbed by unwanted phenomena.

The processing chain includes several steps:

1/ As a pre-processing, denoising can reduce the influence of the additive measurement noise. Thus, Lee *et. al* [1] suggest using subspace methods, initially applied for speech enhancement.

2/ Then, as the target and the radar may move from one emitted burst to another, the scatterers are not necessary located at the same range bins in the 2-D signal. If radar and target motions are not compensated, the resulting range-Doppler image is blurred. Therefore, several papers deal with this issue. A survey about target motion compensation including "range alignment" and "phase compensation" can be found in [2].

3/ Spectrum analysis plays a key role to get the range-Doppler image in ISAR processing. In [3]-[5], the authors focus their attention on this issue and the time-frequency analysis.

4/ In [6], a principal component analysis (PCA) allows the 3-D rotational motion to be detected to deduce information about the relative position of the different target scatterers. This method can be used to avoid blurred image formation. In [7], the so-called quadratic target motion[1] is also compensated.

5/ Among the post-processing helping the practitioner for ship recognition, image processing can be done such as anisotropic diffusion, edge detection, etc.

In this paper, we propose to study the relevance of interpolation techniques for ISAR range-Doppler image post-processing. This can be useful for the practitioner especially when zooming. Our contribution is twofold:

[1] The so-called target quadratic motion is due to the target acceleration.

1/ We propose a variant of the Hölderian regularity-based image interpolation, initially proposed in [8] by two of the authors, Legrand and Levy-Vehel, and studied on images such as the well-known "Lena" image and a Japanese door. It should be noted that smooth regions and irregular ones such as sharp edges and textures remain after zooming. In the original method and the new variant, interpolating consists in adding a new scale in the wavelet transform. The new wavelet coefficients can be deduced from others. However, the variant has the advantage of preserving the signal local regularity.

2/ We compare this approach with several kinds of interpolation methods such as the linear interpolation, the bicubic one, the nearest neighbour interpolation, etc. Synthetic data and real ship range-Doppler images are considered.

The remainder of this paper is organized as follows: in section 2, we introduce the Hölderian regularity-based approach proposed in [8]. Then, we present the variant in section 3. Section 4 deals with the comparative study. Then, conclusions and perspectives are given.

2. Hölderian regularity-based image interpolation

In [8], the authors suggested finding an interpolation technique allowing smooth regions and irregular ones to be preserved. This was reformulated as a constraint on the local regularity of the signal to be preserved. In this section, we first define the local regularity of a signal. Then, we present what the Hölder exponent is and how to obtain it by using the wavelet transform. Then, the Hölderian regularity-based interpolation initially proposed in [9] is briefly recalled.

2.1. Local regularity and Hölder exponent

The local regularity notion is a generalization of function regularity (i.e. continuity and derivability) with non-entire values. If the signal f is continuous in t_0, the local regularity in t_0 is equal or higher than 0. In addition, if the signal f is derivable in t_0, the local regularity in t_0 is equal or higher than 1. Therefore, a large local regularity corresponds to a "smooth" signal, whereas a small local regularity leads to an "irregular" signal.

Let us introduce the Hölder exponent α in t_0 that can characterize the local regularity. In the following, we will say that "$f \in C^{\varepsilon}(t_0)$", with $\varepsilon > 0$, if one can find constants $C > 0$, $\delta > 0$ and a polynomial P, the degree of which is lower than n, such as :

$$\text{if } |t - t_0| \le \delta \text{, then } |f(t) - P(t - t_0)| \le C|t - t_0|^n \qquad (1)$$

The above property is verified for a continuum of ε. Then, the Hölder exponent α of the function f in t_0 is defined as the supremum value of ε satisfying the above property (1):

$$\alpha = \sup_{\varepsilon}\left(f \in C^{\varepsilon}(t_0)\right) \qquad (2)$$

Then, the Hölder exponent is the maximal local regularity of the function f in t_0.

2.2. Local Regularity and wavelet coefficients [9]

Let f denote the input signal of length N and let $c_{m,n}$ be its wavelet coefficients, where m corresponds to the scale and n to the time. See appendix A for details on the wavelet transform.

If f is a uniform Hölderian signal[2], then a constant $c > 0$ exists so that the wavelet coefficients satisfy [10]:

$$\forall (m,n) \in \boldsymbol{Z}^2, \quad |c_{m,n}| \le c 2^{-m\left(\alpha + \frac{1}{2}\right)} \left(1 + \left|2^l . t_0 - n\right|\right)^{\alpha} \qquad (3)$$

Reciprocally, for any $\alpha' < \alpha$:

$$\text{if } \forall (m,n) \in \boldsymbol{Z}^2, \text{ we have } |c_{m,n}| \le c 2^{-m\left(\alpha + \frac{1}{2}\right)} \left(1 + \left|2^m . t_0 - n\right|\right)^{\alpha'}$$

Then, the Hölder exponent of the function f in t_0 is α.

According to equ. (3), the wavelet-coefficient absolute values in the cone of influence [3] are bounded by a term which depends on the Hölderian exponent.

If we restraint to the wavelet coefficients in the cone of influence, then these coefficients are supposed to be nearly equal to $2^{-(\log_2(N) - m + 1)\left(\alpha + \frac{1}{2}\right)}$. Consequently, one has:

$$\log_2 |c_{m,n(m,t_0)}| = -(\log_2(N) - m + 1)\left(\alpha + \frac{1}{2}\right) \qquad (4)$$

Under this assumption, the Hölder exponent can be estimated by searching the slope s of the regression line of $\left\{\log_2 |c_{m,n}|\right\}_{m=1,\cdots,\log_2(N),\, n=1,\cdots N \times 2^{-m}}$ according to the scale $\left\{(\log_2(N) - m + 1)\right\}_{m=1,\cdots,\log_2(N)}$:

$$\alpha = -s - \frac{1}{2} \qquad (5)$$

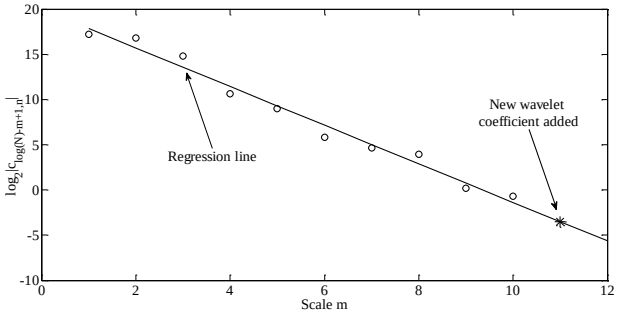

Fig. 1. Linear regression of wavelet coefficients

---

2 f is a uniform Hölderian signal if one can find constant $\varepsilon > 0$, such as $f \in C^{\varepsilon}(\boldsymbol{R})$, where $\boldsymbol{R}$ denotes to the set of the real numbers. (whereas $\boldsymbol{Z}$ refers to the set of the integer numbers).

3 If ψ has a compact support, the cone of influence of t_0 in the time-scale plane is defined in [11] as the set of points (a,b) such as t_0 is included in the support of $\psi_{a,b}(t) = \frac{1}{\sqrt{a}}\psi\left(\frac{t-b}{a}\right)$.

If ψ has a compact support equal to $[-K,K]$, the support of $\psi\left(\frac{t-b}{a}\right)$ is equal to $[b - Ka, b + Ka]$, and the cone of influence of t_0 is defined by : $|b - t_0| \le Ks$.

2.3. Signal interpolation method

Given sections 2.1 and 2.2., the interpolation method initially proposed in [8] operates into four steps:

1/ A wavelet transform of the signal, which has to be interpolated, is done.

2/ According to the sub-section 2.2, the signal local regularity in t_0 is estimated by searching the slope s of the regression line of $\left\{\log_2\left|c_{m,n(m,t_0)}\right|\right\}_{m \text{ and } n \text{ in the cone of influence in } t0}$ versus the scale $\left\{(\log_2(N)-m+1)\right\}_{m=1,\cdots,\log_2(N)}$. This regression slope provides local-regularity information. See Fig. 1.

3/ A new wavelet coefficient (denoted by a cross $*$ on Fig. 1) is introduced such as the logarithm of the absolute values of this wavelet coefficient is on the regression line.

4/ The interpolated signal is reconstructed by making an inverse wavelet transform.

These steps are repeated $\frac{N}{2}$ times as shown in Fig. 2.

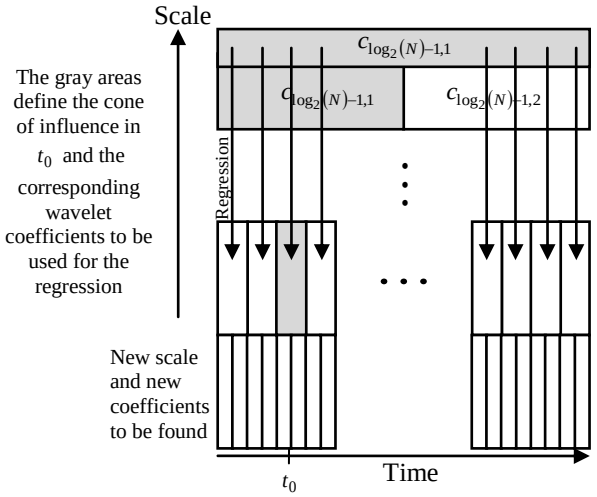

Fig. 2. Interpolation principle based on the dyadic grid

It should be noted that this method can be repeated to interpolate as many times as the user wants.

However, only the absolute value of the new wavelet coefficient is obtained and the coefficient sign is unknown. In [9], the authors suggest choosing the opposite of the sign of the previous-scale wavelet coefficient.

This method makes it possible to take into account the interpolated signal regularity and the reconstruction error. Both properties have practical importance: the regularity determines added-information visual appearance (i.e. the high frequencies content) whereas the interpolation convergence means that the added information is not "very" different from the reality.

2.4. Image interpolation method

To interpolate an image, the extension of the above method to the 2D case cannot be considered because diagonal interpolation would use pixels which are not near to the pixel of interest.

Therefore, an alternative consists in using the method presented in section 2.3 to first interpolate the rows and then deduce the columns of the image. Nevertheless, the 1-D interpolation method is not used for diagonal interpolation. In [9], these diagonal points are calculated as the mean of the adjacent original and interpolated points. See Fig. 3. In addition, the Haar wavelet is used to obtain the same result for the signals $\{z(n)\}_{n=1,\cdots,N}$ and $\{z(N-n+1)\}_{n=1,\cdots,N}$. Thus, when dealing with a row or a column of pixel in an image, our purpose is to obtain the same interpolation when the image is flipped horizontally or/and vertically.

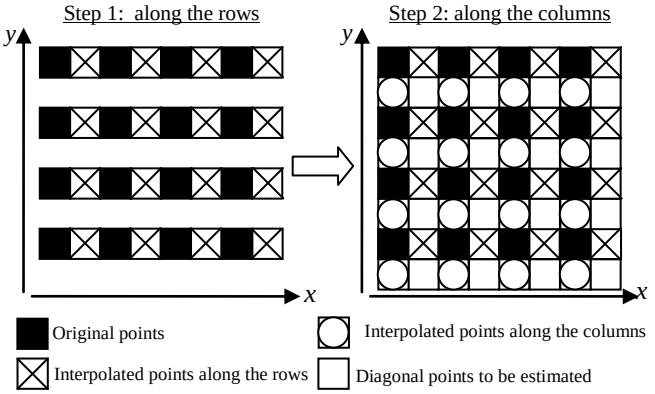

Fig. 3. Image interpolation method

3. Hölderian regularity-based image interpolation variant

The drawback of the above image interpolation method is that the diagonal-point interpolation does not conserve the Hölderian regularity. Consequently, we propose a new approach to interpolate the diagonal points. It is based on the estimation of the local orientation, with a tensor structure [12] for instance.

For each diagonal point, the four adjacent points of the original image are considered. See Fig. 4. Then, the gradient field is calculated on these four points:

$$\overrightarrow{\nabla I}(i)=\left(G_x(i),G_y(i)\right)^T \qquad i=1,\cdots,4 \tag{6}$$

where the upperscript ^{T} denotes the transpose and G_x (resp. G_y) is the gradient according to the x-axis (resp. y-axis).

Then, the 2×2 covariance matrix of the gradient T is defined by:

$$T=\begin{bmatrix} \sum_{i=1}^{4} G_x(i)^2 & \sum_{i=1}^{4} G_x(i)G_y(i) \\ \sum_{i=1}^{4} G_x(i)G_y(i) & \sum_{i=1}^{4} G_y(i)^2 \end{bmatrix} \tag{7}$$

At that stage, a principal component analysis on T provides the orientation θ defined by the eigenvector associated to the predominant eigenvalue. This orientation is used to determine the diagonal-point interpolation.

The diagonal-point can be interpolated as follows (see Fig. 4):

1/ after the interpolation along the rows and the columns, a new interpolation can be done on the interpolated pixels. It provides a first interpolated diagonal pixel (represented by a cross ⊠ on the Fig. 4) if one uses the interpolated row pixels or another interpolation (represented by a circle ◎ on the Fig. 4) if one uses the interpolated column pixels.

2/ A weighted average of both values is done to obtain the value of diagonal-point. Note that the weights depend on the orientation θ.

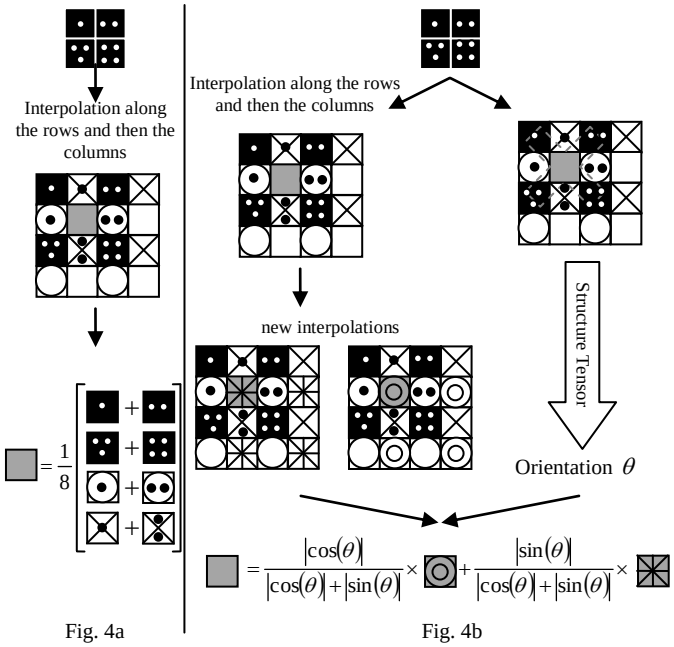

Fig. 4a Fig. 4b

Fig. 4. Diagonal point estimation
in the original method [9] (Fig. 4a) and the variant (Fig.4b)

4. Comparative study

We propose to evaluate the interpolation methods on synthetic data and real range-Doppler image. A comparative study is carried out between the linear interpolation, the bicubic one, the nearest neighbour interpolation, the approach proposed in [8] and our variant.

The test image is given on Fig. 5a. On the Fig. 5b-f, the image is interpolated three times with various methods. As we can see, two methods provide clear interpolated images: the nearest neighbour interpolation and our approach.

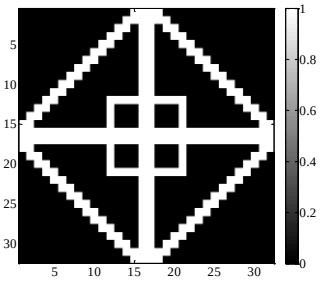

Fig. 5a
original image

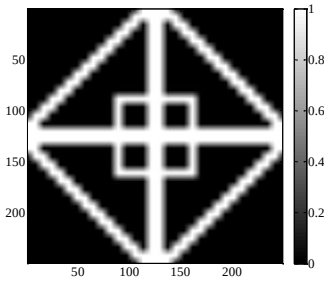

Fig. 5b
linear interpolation

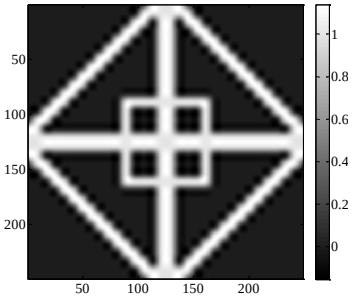

Fig. 5c
bicubic interpolation

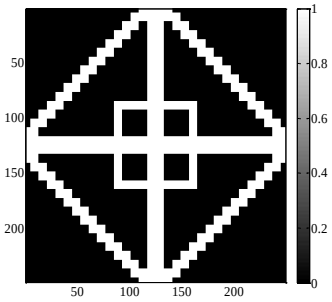

Fig 5d
nearest neighbour

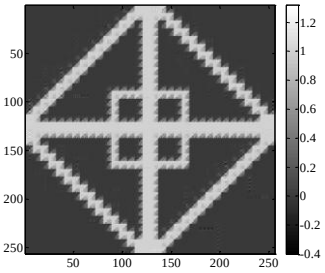

Fig. 5e
Legrand and Levy-Vehel [8]

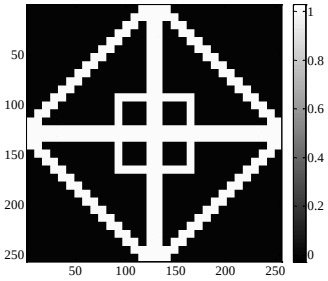

Fig. 5f
our method

Fig. 5. Image interpolation on a synthetic image

Let us now the real range-Doppler image. Due to its size, we propose to compare the methods on two-time-interpolated images. We present a global view of the image and then we zoom with the different interpolation algorithms.

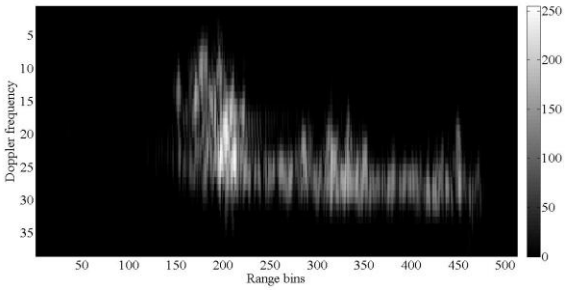

Fig. 6 Original ISAR image

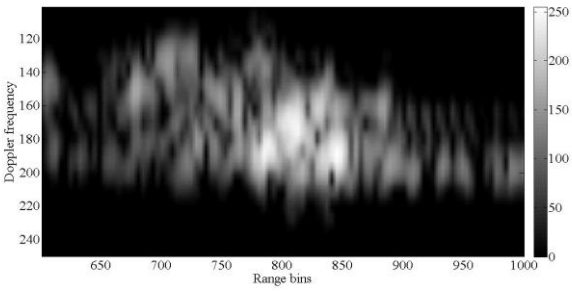

Fig. 7a. Linear interpolation which smoothes the most among the tested interpolation techniques

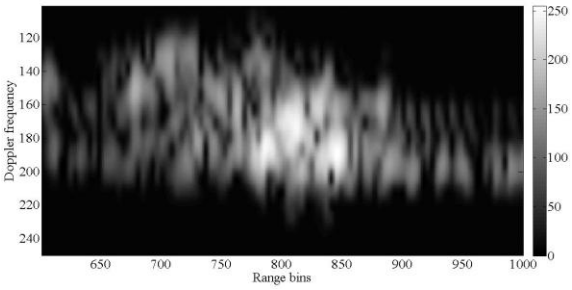

Fig. 7b. Bicubic interpolation

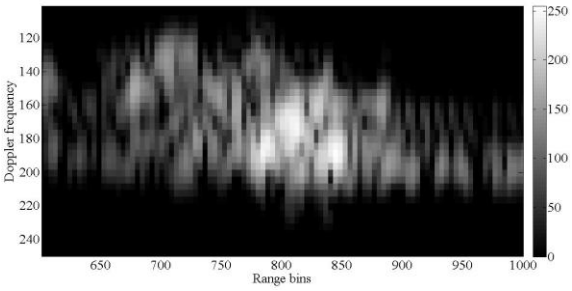

Fig. 7c. Nearest neighbour interpolation

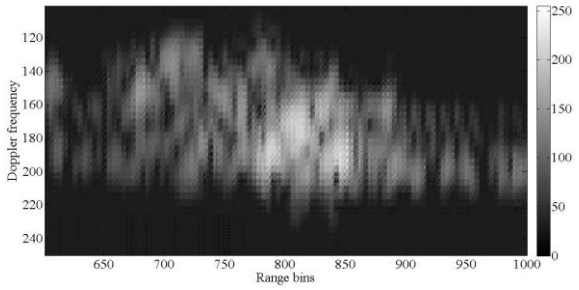

Fig. 7d. Levy-Vehel's method [8]

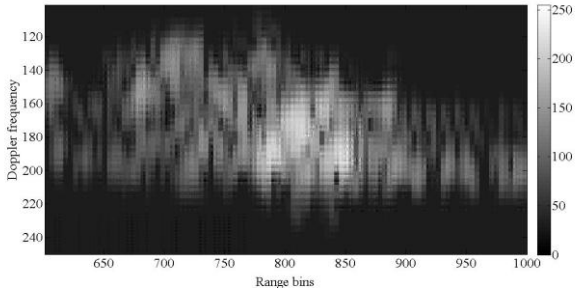

Fig. 7e. Our variant that smoothes less than the other methods

5. Conclusions

The practitioner can use several kinds of interpolations for ISAR post processing. The simulation results confirm the effectiveness of the new interpolation approach both for the synthetic data and range Doppler ISAR image.

Acknowledgements

The authors would like to thank Thales Airborne Systems from providing us with real ship range-Doppler images, recorded as part of Thales program.

Appendix A

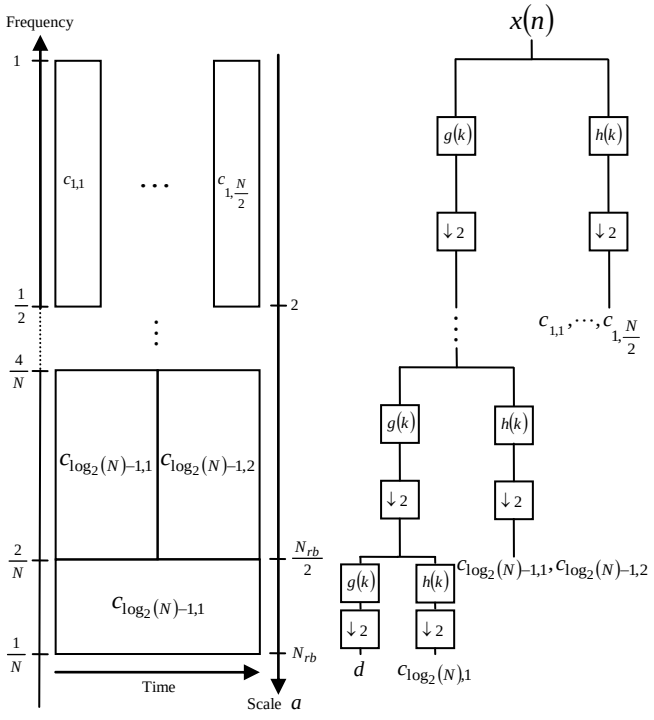

Fig.6. Dyadic grid and filter bank for multi-resolution decomposition of $x(t)$

The discrete standard wavelet transform is a well-known tool to capture both time and frequency information. The wavelet transform is the projection on the sliding windowed functions $\psi_{a,b}(t)$ of a given signal x of length N ($\log_2(N)$ is an integer):

$$\psi_{a,b}(t)=\frac{1}{\sqrt{a}}\psi\left(\frac{t-b}{a}\right) \tag{8}$$

where ψ is called the mother wavelet, j the scale factor and k the translation factor. To reduce the computational cost and the redundancy, a discretization of the scale and translation factors can be done and leads us to a dyadic grid: $a=2^m$, $b=n.2^m$ with $m=1,\cdots,\log_2(N)$ and $n=1,\cdots,N\times 2^{-m}$

From the point of view of implementation, at each decomposition level of the discrete wavelet transform, the signal $x(t)$ is filtered by two filters, a high-pass filter $h(k)$ and a low-pass filter $g(k)$. Both filter outputs are then downsampled by a factor of 2 and produce respectively low-pass and highpass subband outputs, which corresponds to the smoothed version of the signal and signal details. Due to the downsampling, the number of resulting wavelet coefficients $c_{m,n}$ is exactly the same as the number of input points N.

References

[1] K.-C. Lee, J.-S. Ou and M.-C. Fang, "Application of SVD Noise-Reduction Technique to PCA Based Radar Target Recognition," Progress in Electromagnetics Research, pp. 447-459, 2008.

[2] J. Wang and X. Liu, "Improved Global Range Alignment for ISAR," IEEE Trans. on Aerospace and Electronic Systems, Vol. 43, n°3, pp. 1070-1075, 2007.

[3] V. Popovic, T. Thayaparan and L. Stankovic, "Noise Analysis of the High Resolution Methods in ISAR," Proceedings of International Symposium on Image and Signal Processing and Analysis, pp. 489-493, 2005.

[4] V. C. Chen and S. Qian, "Joint Time-Frequency Transform for Radar Range-Doppler Imaging," IEEE Trans. on Aerospace and Electronic Systems, Vol. 34, n°2, pp. 486-499, 1998.

[5] L. Stankovic, T. Thayaparan, V. Popovic, I. Djurovic and M. Dakovic, "Adaptive S-Method for SAR/ISAR Imaging," EURASIP Journal on Advances in Signal Processing, Vol. 2008, n°2, 2008.

[6] W. Nel, D. Stanton and M. Gaffar, "Detecting 3-D Rotational Motion And Extracting Target Information From The Principal Component Analysis of Scatterer Range Histories," Proceedings of International Radar Conference, 2009.

[7] T. Thayaparan, L. Stankovic, M. Dakovic, I. Djurovic and V. Popovic, "Image Enhancement and Motion Compensation of Moving Targets in ISAR using S-Method", Proceedings of IEEE International Radar Conference, 2009.

[8] J. Levy-Vehel and P. Legrand, "Hölderian Regularity-Based Image Interpolation," Proceedings of the IEEE ICASSP, Vol. 3, 2006.

[9] Legrand P., "Débruitage et Interpolation par Analyse de la régularité Höldérienne. Application à la modélisation du frottement pneumatique-chaussée," PhD in French supervised by J. Levy-Vehel, 2004.

[10] S. Jaffard, "Wavelet Techniques in Multifractal Analysis," Proceedings of Symposia in Pure Mathematica, Vol. 72, n°2, pp. 91-152, 2004.

[11] S. Mallat, *A Wavelet Tour of Signal Processing*, Academic Press, 1998.

[12] J. Bigün and G. Granlund, "Optimal Orientation Detection of Linear Symmetry," Proceedings of the 1st International Conference on Computer Vision, pp. 433-438, 1987.